This paper was awarded in the I International Competition (1992/93) "First Step to Nobel Prize in Physics" and published in the competition proceedings (*Acta Phys. Pol. A* **85** Supplement, S-13 (1994)).
The paper is reproduced here due to kind agreement of the Editorial Board of "Acta Physica Polonica A".

# BETA BACKSCATTERING BY METALLIC ELEMENTS AND SIMPLE COMPOUNDS

## I. Galloway

**George Watson's College, Colinton Road, Edinburgh, Scotland, Great Britain**

The aim was to investigate the angular dependence of the $\beta$-particle backscatter count rate, using a strontium-90 source. In addition the empirical relationship between the atomic number ($Z$ number) of a scatterer and the count rate at a specific angle was investigated along with consideration of how this relationship behaves with simple compounds. Thick samples are used throughout. A brief investigation of counting statistics is included as an appendix.
PACS numbers: 34.80.−i

## 1. Introduction

### 1.1. Backscattering Theory and its Applications

When a $\beta$-particle enters a material its path can be deflected when it interacts with the nuclei of the material. The $\beta$-particles are oppositely charged to the positively charged nucleus and thus an attractive force exists between the two. The deflections that result are dependent on the initial energy of the $\beta$-particles but the effect is of a general *scattering* of the particles. This usually has the effect of changing the forward direction of a $\beta$-particle by a few degrees, but occasionally if the $\beta$-particle is suitably orientated in relation to the nucleus, the $\beta$ will be deflected through a value of around 180° resulting in it exiting the material from the same side as it entered [1]. It is this phenomenon that is known as *backscattering*.

For thick samples, as yet no theoretical relationship exists on $\beta$-particle backscattering due to the complexities of calculations involving multiple scattering. That is to say when a $\beta$-particle enters a material it may scatter off many different atoms before leaving the material and thus the idea of backscattering being uniquely an interaction between one $\beta$-particle and one atom breaks down. In certain cases relationships developed to deal with single scattering can be used as a possible approximation to what is actually happening. In any case the relationships that do exist concerning backscattering are purely empirical.

Beta particle backscattering has been a subject for investigation for many years; yet data, theoretical or experimental, on any relationships between atomic number ($Z$ number) of the scatterer, the angle of scattering and the count rate, is sparse. The subject has been mainly of interest to physicists involved in the laws of charged particle scattering and those developing devices such as $\beta$-ray thickness gauges.

The recent increase in the availability and use of high-energy electron accelerators has caused a necessity for greater understanding of the above ideas.

Specific examples of the applications are in the use of radiation therapy for the treatment of tumours and in Computer Aided Tomography Scanners (more commonly known as CAT scanners). Understanding $\beta$-ray backscattering becomes useful in attempting to target tumours with greater accuracy and in the optimal use of data gained from CAT scanners. This is due to the fact that the density of tissue is far from even throughout the human body and at high/low density boundaries $\beta$-ray backscattering becomes a significant factor in determining the absorbed dose of the surrounding tissues. Unfortunately due to theoretical complexities no satisfactory theoretical solution to the practical application of $\beta$-ray backscattering has as yet been published.

## 2. Initial data

Before the main aims of the investigation can be tackled there are a few preliminary experiments that have to be completed to give information on the equipment and source that it is proposed to use. In many cases in this investigation the raw data obtained is itself of little interest. In this circumstance only the graphs of the data have been included.

### 2.1. Transmission through air of a collimated $\beta$ source (Sr-90)

This experiment was to determine the order of the size of separations that could be used between the source/scatterer and scatterer/Geiger Müller (G–M) tube. From the graph of this data (Fig. 1) it can quite clearly be seen that once the distance between the source and the detector has exceeded approximately 0.40 m the count rate has fallen almost onto the $x$-axis. Such separations are therefore not acceptable as there are not a significant number of $\beta$-particles to count. In addition if the total separation is less than approximately 0.05 m the number of counts per minute changes so rapidly with the separation that there is an excessive error in the count due to any error in positioning. For accurate results in the further experiments it would be wise to keep the total distance between source and detector to a value inside these limits.

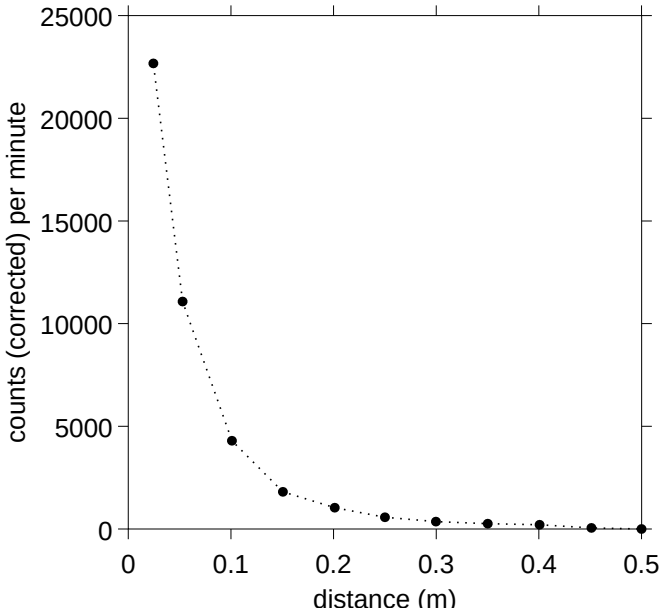


**Fig. 1.** A plot of the transmission of $\beta$-particles through air. The errors in the data are not indicated as error bars as such, since the data points on the graph exceed the error bars in their diameter.

This graph is used in later experiments to estimate the counting error due to any error in the distance between the source and the G–M tube. See Appendix A for a

further explanation of errors.

The fall in the count rate as the source/detector separation increases is possibly due to the scattering of the $\beta$-particles as they travel through the air. Assuming that the source is perfectly collimated we would expect the following relationship, based on the theoretical idea of scattering in Fig. 2:

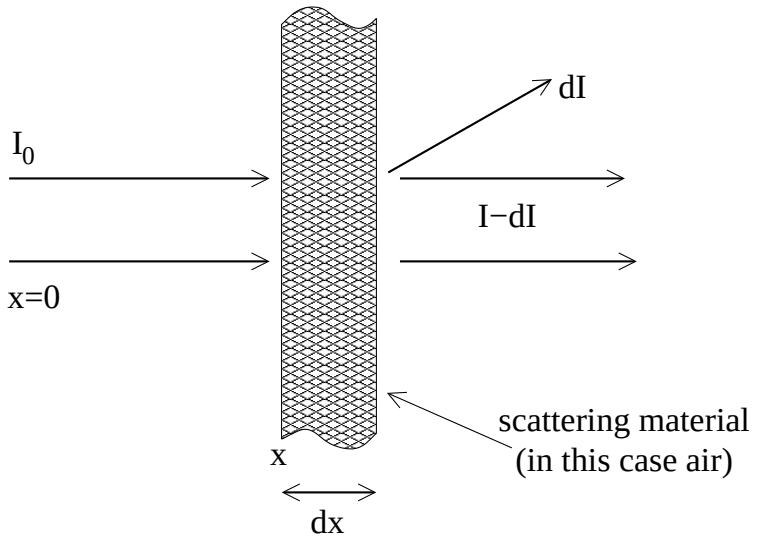


**Fig. 2.** The scattering of $\beta$-particles as they pass through a material.

$$-\mathrm{d}I \propto I\mathrm{d}x \Rightarrow cI = \mathrm{e}^{-\mu x},$$

$$I = I_0 \quad \text{at} \quad x = 0 \Rightarrow c = 1/I_0,$$

therefore

$$I = I_0\mathrm{e}^{-\mu x}. \tag{1}$$

As formula (1) suggests the relationship between count rate and distance is indeed an exponential decay but as can be seen from the graph (Fig. 3) the decay is not just one exponential curve but two. This is very probably the result of the two-stage decay process of strontium-90, shown below [2]

$$^{90}\mathrm{Sr} \rightarrow ^{90}\mathrm{Y} + \beta^- \ (0.5 \text{ MeV}),$$

$$^{90}\mathrm{Y} \rightarrow ^{90}\mathrm{Zr} + \beta^- \ (2.2 \text{ MeV}).$$

The $\beta$ decay process gives out a spectrum of $\beta$ energies with a finite limit that depends upon the element and thus having two $\beta$ decays provides two separate spectra of $\beta$-particle energies. Therefore the two different maximum energies will be predominant in affecting the transmission at different distances and thus possessing different values of $\mu$, the scattering coefficient.

### 2.2. Variation of count rate with angle of detection

Another important factor to investigate was the imperfection of the collimated beam of the $\beta$ source. The procedure was to record the count rate at a fixed distance from the source and to vary the angle $\theta$ from the normal at which the readings are taken. A diagram of the experimental set-up is shown in Fig. 4 with the graph of the results in Fig. 5.

Due to the reasonably large spread in angle which is detected by the G–M tube this source is reasonably well collimated.

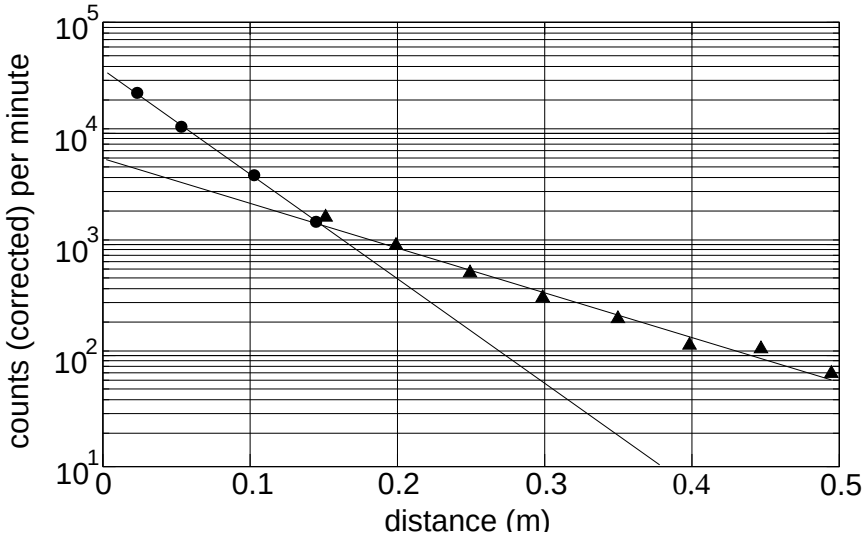


**Fig. 3.** A plot of the transmission through air of a collimated $\beta$ source. The errors in the data are not indicated as error bars as such, since the data points on the graph exceed the error bars in their diameter. The lines drawn are the regression lines of the two sets of data points. (A straight line on a logarithmic axis demonstrates that the data points do indeed fit an exponential decay.) The steeper line is probably due to the lower maximum $\beta$ energy (0.5 MeV) of the $^{90}$Sr, with the line of lesser gradient being attributed to the higher maximum $\beta$ energy (2.2 MeV) of the $^{90}$Y. The lesser $\beta$ energies of the $^{90}$Sr will mean that it is scattered much more by the air and thus its effect will die out quickly leaving the effects of the higher energy $\beta$-particles of the $^{90}$Y at larger distances.

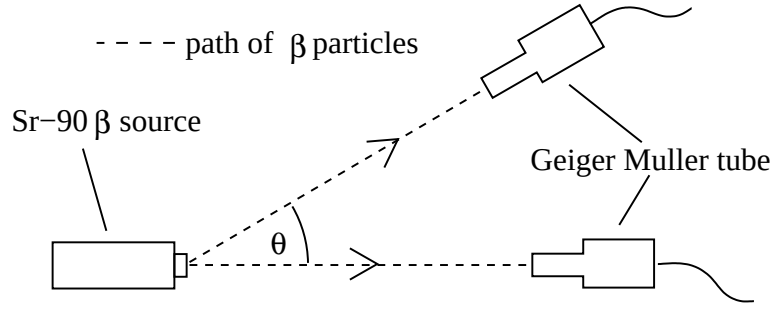


**Fig. 4.** The experimental set-up while measuring the relationship between angle of detection and the variation in the count rate.

## 3. Angular dependence of $\beta$ scattering

The initial experiments were carried out using aluminium with the experimental set-up shown in Fig. 6 [3].

### 3.1. $\beta$-particle backscattering with aluminium

The initial data collected (Table I) was of more qualitative than quantitative value, as it became apparent that the count rates were not significant in comparison to the background rates. All the counts were measured over 180 seconds.

There were a few solutions to the problem. Firstly, if the total source/detector separation was reduced then the count rate should increase considerably (based on the ideas developed earlier concerning the scattering of $\beta$-particles through air and the imperfections of the collimated beam). Due to the rather bulky shapes of source holder, a clamp stands and the detector, a 10° measurement would no longer be possible if the apparatus was moved closer together. The other main option was to change the scattering material

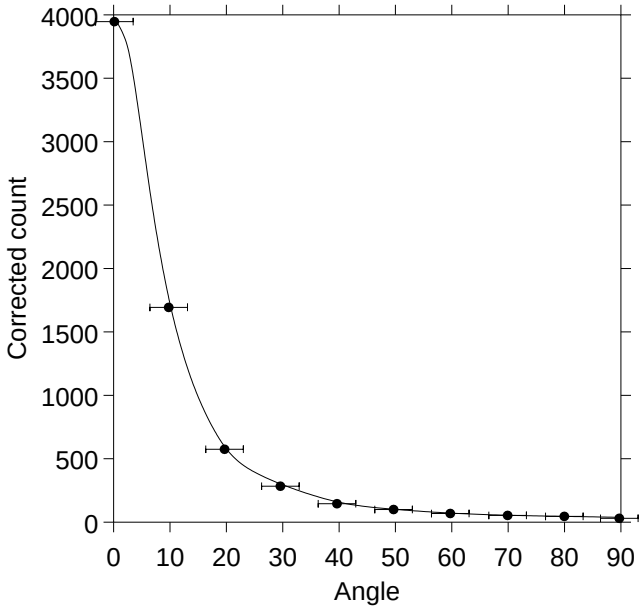


**Fig. 5.** A plot of the count rate against the angle of detection. The points plotted on the graph exceed the vertical error bars in their diameter and thus no vertical error bars are shown.

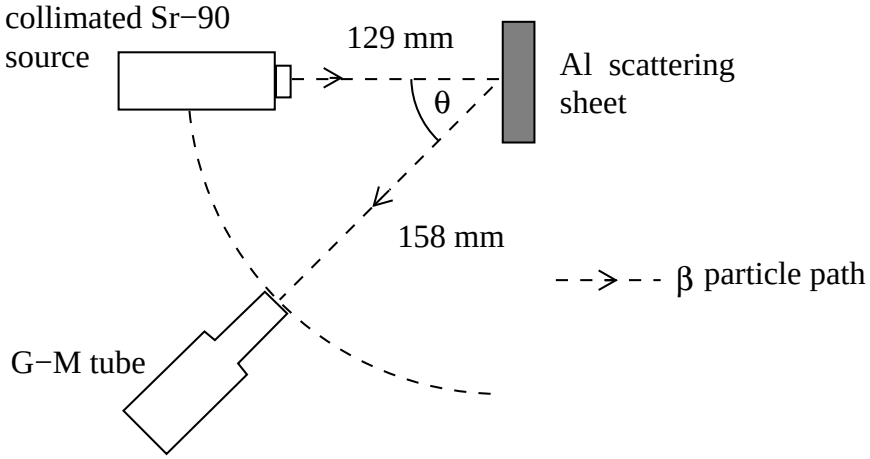


**Fig. 6.** The experimental set-up while measuring the relationship between angle of detection and backscatter count rate.

TABLE I. Aluminium backscattering.

| Background | Al sheet thickness [mm] | Angle $\theta$ | Count |
|---|---|---|---|
| 2.03 | 10° | 193 | 174 |
| 2.03 | 20° | 124 | 149 |
| 2.03 | 30° | 111 | 111 |
| 2.03 | 40° | 95 | 75 |
| 50.00 | 10° | 175 | as above |
| 50.00 | 20° | 116 | as above |

to something with a higher atomic number, which according to theory, should scatter a greater proportion of $\beta$-particles and thus increase the counting rate. It was the latter of these two options that was chosen first.

### 3.2. $\beta$-particle backscattering with lead

The experimental set-up was only changed from the previous experiment with alu-

minium by the following:

- – The scatter was changed to a lead block 12.5 mm thick;
- – A lead block was placed between the source and the G–M tube to act as shielding (this was not sufficient on its own to enable counting with Al);
- – The source/scatterer distance was 129 mm;
- – The scatterer/G–M tube distance was 158 mm.

The angular dependence of backscattering could be seen with this set-up but the errors were too great to conclude reliably any more than this. The experiment was repeated but this time the total distance that a $\beta$-particle had to travel was substantially reduced. As the apparatus was so much closer together no measurement could be taken for an angle of 10°. The source/lead scatterer distance was 55 mm; the scatterer/G–M tube distance was 60 mm. The graph (Fig. 7) was obtained from the results. The duration of each count was 300 seconds.

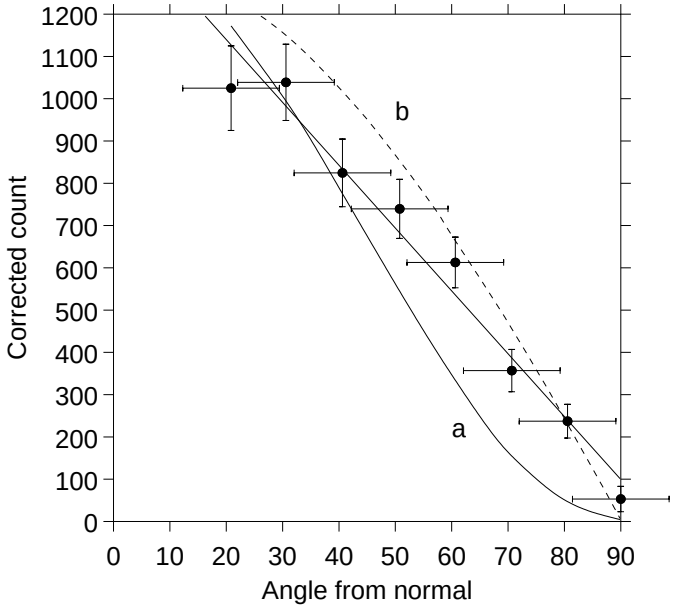


**Fig. 7.** A plot of the backscatter count rate against the angle of detection (taken from the normal) with a lead sample. Included is a linear regression line and the empirical boundaries into which points are expected to fall. These are of the form: (a) $y = k\cos^2 x$, (b) $y = k\cos x$. The error in the angle $\theta$ is the maximum error in the angle. This error is due to the wide radius of the G–M tube but as it is circular the G–M tube will count fewer $\beta$-particles at the edge of the tube. Therefore the error is not uniform but the maximum possible error.

The points on the graph are bounded by two curves of the form

$$y = k\cos x \quad \text{and} \quad y = k\cos^2 x.$$

This type of fit is suggested from empirical data by Knop and Paul [4].

The value of the constant $k$ in the figure is chosen approximately, determined from the fit of the data of Knop and Paul to the curves. Thus the above curves should relate as closely as possible to the data in this experiment.

Another set of results was obtained to check the repeatability of the experiment and thus the validity of the conclusions. The graph of the results is shown in Fig. 8. The counts were measured over 180 seconds.

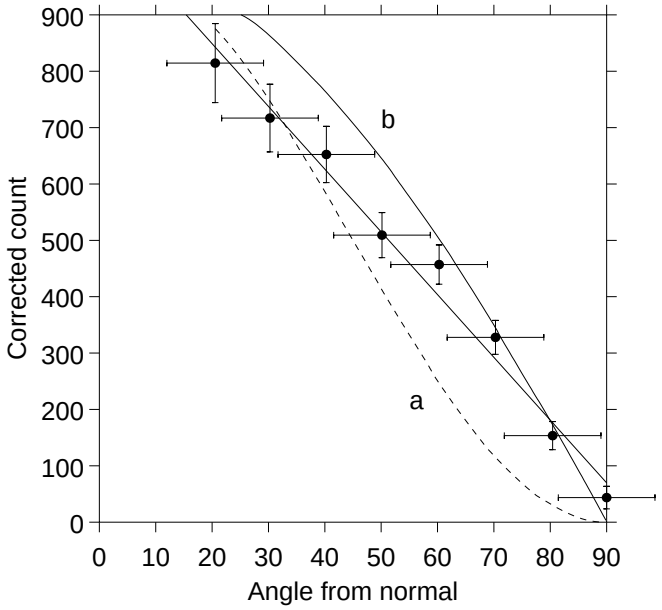


**Fig. 8.** A second plot of the backscatter count rate against the angle of detection (taken from the normal) with a lead sample. The sample boundaries are included as in Fig. 7.

As can be seen from both of these graphs of $\beta$ backscattering against angle, although the points fit reasonably well inside the limits set by the cos and $\cos^2$ curves they actually fit a linear equation much more accurately (seen from the points' proximity to the linear regression line).

A simplified formula for the backscattering of mono-energetic electrons was given by Bethe et al. [5]

$$I = (0.717 + \cos\theta)\cos\theta.$$

An interesting result is discovered if a graph of this formula is drawn and the line of best fit found for the data range used in the last two experiments ($20° < \theta < 90°$). What is found, shown in Fig. 9, is that the points lie very close to a straight line compared with the range given by the cosine estimates. This is purely a qualitative observation but it illustrates clearly that although the small amount of research that exists suggests that the data should follow some sort of cosine or cosine squared fit, over the range that was used in the experiments in this investigation, the fit is very nearly linear. It can therefore be said with some certainty that there does exist an approximately linear relationship between the count rate and the backscattered angle over the range $20° < \theta < 90°$.

## 4. Atomic number dependence

As has already been suggested there is a connection between the atomic number ($Z$ number) of an element and its ability to produce high $\beta$ backscatter count rates. These ideas were tested using equipment in the University of Edinburgh's First Year Physics teaching laboratories. The experimental set-up is shown in Fig. 10.

The samples that were initially used for backscattering were cylinders of approximately equal diameter of the following elements: carbon, aluminium, iron, copper, indium, tin, tungsten, lead. Similar cylinders of polythene ($\sim CH_2CH_2\ \sim$), iron oxide, potassium chloride, sand ($SiO_2$) and glass (taken as $SiO_2$) were also used at this stage to see how simple compounds might fit the relationship.

Previous work on this topic has suggested an empirical linear relationship between the count rate and $\log(Z)$. In addition Baily (1980) [6] found that much backscattering data

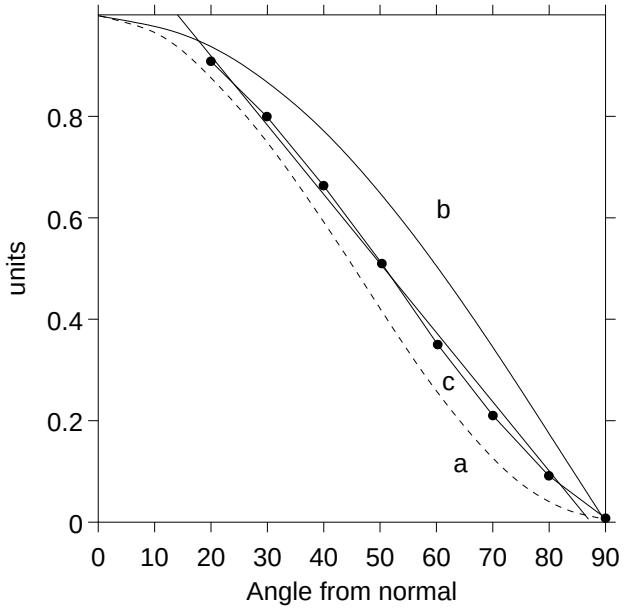


**Fig. 9.** This graph demonstrates the good approximation to a linear fit that the Bethe equation gives over the range $20° < \theta < 90°$. A linear regression line of the points is shown along with: (a) $y = \cos^2 x$, (b) $y = \cos x$, (c) $y = [(0.717 + \cos x)\cos x]/1.717$.

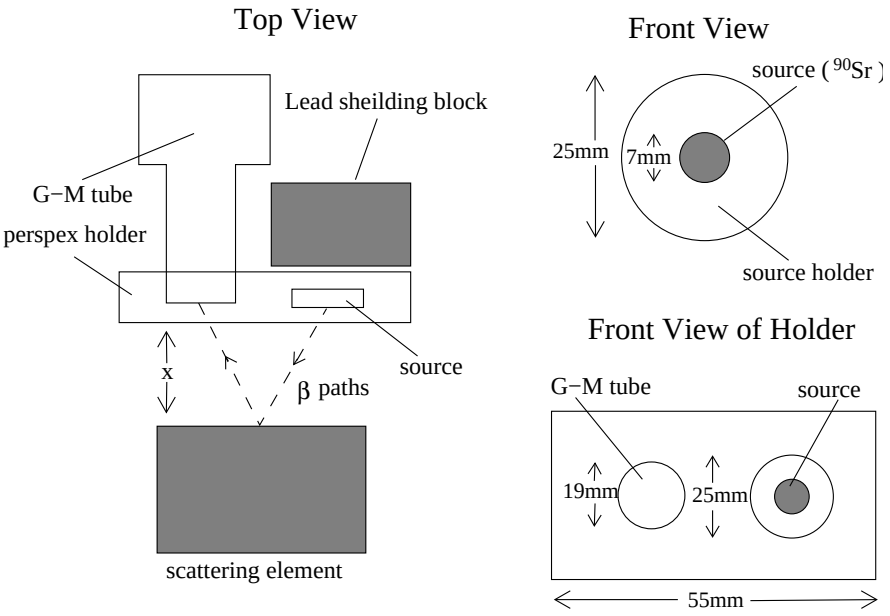


**Fig. 10.** A diagrammatic representation of the first experimental set-up while measuring the atomic number dependence of $\beta$-particle backscattering.

could be fitted empirically with a $\log(Z + 1)$ dependence. An approximation to $\log(Z)$ for compounds is calculated as the sum of the relative proportions of each constituent element multiplied by the logarithm of its atomic number. A similar calculation is used for an approximation to $\log(Z + 1)$. After briefly testing the experimental set-up to see if some sort of relationship was visible from the results the tin cylinder was arbitrarily chosen to find the optimum distance from the source to achieve the highest count rate. It can quite clearly be seen from the diagrams in Fig. 10 that if the scatterer was placed too close to the source/G–M tube holder virtually no $\beta$-particles would be able to enter the G–M tube from the scatterer. Also if the scatterer is too far away from the source and G–M tube, the $\beta$-particles will be scattered by the air; thus there must be an optimum separation.

TABLE II. Optimum separation for $Z$ dependence measurements.

| Separation [mm] | Count |
|---|---|
| 8 | 419 |
| 11 | 492 |
| 12 | 463 |
| 13 | 507 |
| 14 | 488 |
| 15 | 443 |
| 18 | 424 |
| 23 | 367 |
| 28 | 288 |
| 33 | 269 |
| 38 | 178 |

Table II shows that the highest count is with a separation of $x = 13$ mm. As the most accurate measurement that can be made is $\pm 0.5$ mm it is quite acceptable to use 13 mm as the optimum separation without drawing a graph of the results. This separation is used in all further experiments (Figs. 11 to 15). The measurements in the following experiments were taken over 300 seconds.

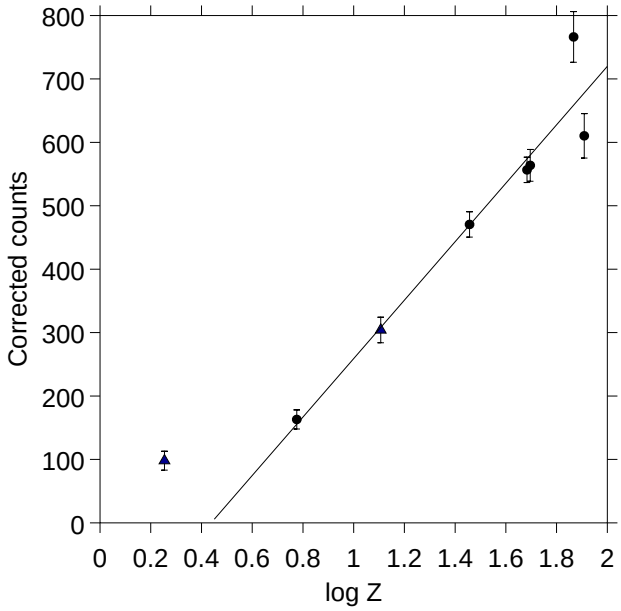


**Fig. 11.** The first plot of the $Z$ dependence of backscattering. The regression line drawn does not include the polythene measurement (furthest left point). It does, however, show a clear linear relationship between the $\log(Z)$ and the count, even although some of the elements with larger atomic number are slightly off the line. Elements are denoted by circles while the polythene measurement is marked as a triangle.

On returning to use the school equipment a new experimental set-up was arranged and all the samples used were in solid form, as opposed to powders. They were: lead, copper, iron, aluminium, phosbronze (92% Cu, 8% Sn), perspex ($\sim CH_2CCH_2COOCH_3\sim$), copper sulphate ($CuSO_4 \cdot 5H_2O$), calcite ($CaCO_3 \cdot 6H_2O$).

Two sets of experimental data were collected and the relevant graphs are shown in the figures. All measurements were taken over 180 seconds. These results (Figs. 14 and 15) used lead, iron, aluminium, phosbronze (92% Cu, 8% Sn), perspex, glass, a copper sulphate crystal ($CuSO_4 \cdot 5H_2O$) and a calcite crystal ($CaCO_3 \cdot 6H_2O$).

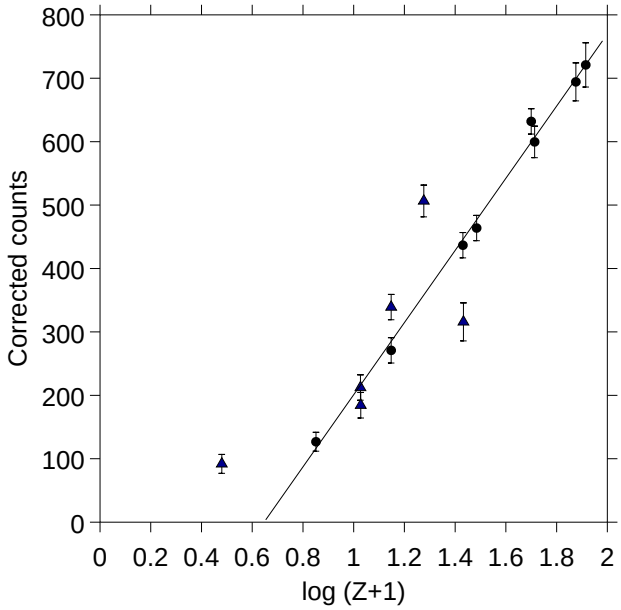


**Fig. 12.** The second plot of the $Z$ dependence of backscattering. Again the regression line drawn is the line of the best fit on the elements only and on this set of results a much better fit is observed with all the points or their error bars lying on the line. Elements are denoted by a circle while compounds are marked by a triangle. The compounds theoretically would be expected to fit reasonably closely to this line but there are a few reasons why they might not. Because the carbon scattering is only slightly above the polythene (the lowest point on the graph with formula $\sim CH_2CH_2\sim$) where the polythene's calculated effective $Z$ number is much lower than that of carbon it is arguable that the hydrogen does not fit the $\log(Z+1)$ relationship (see text). The three compounds which are further away from the line are all powdered samples and their position may depend upon how well the samples were prepared. An answer to this would be to use large solid crystals.

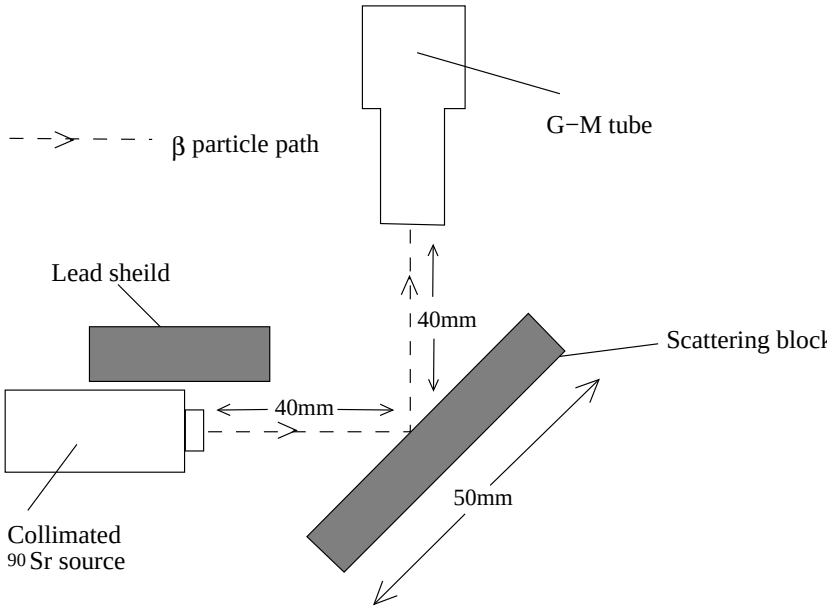


**Fig. 13.** The second experimental set-up while measuring the atomic number dependence of $\beta$-particle backscattering.

The regression lines are drawn through the element points as they seem to give a reasonably consistent line as shown by the graphs in Figs. 11 and 12. This allows

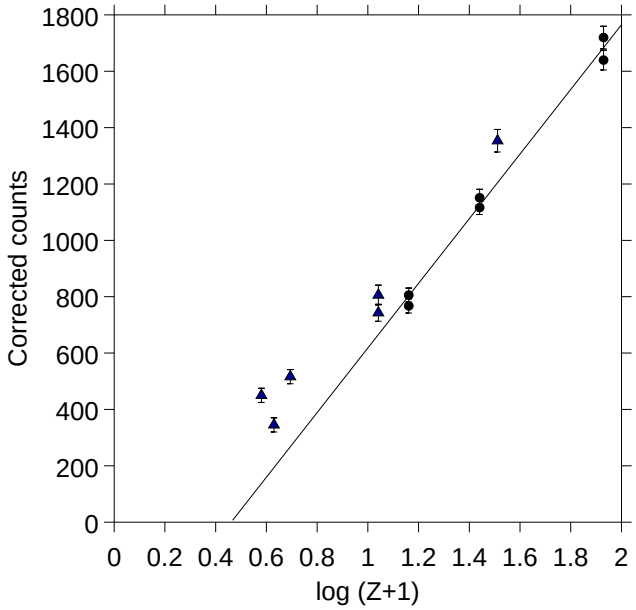


**Fig. 14.** The third plot the $Z$ dependence of backscattering. The regression line drawn is the best fit of the element points only. Elements are denoted by a circle while compounds are marked by a triangle. The lower points on the graph are thought to be off the regression line because of the imperfections of the empirical $\log(Z+1)$ relationship when dealing with hydrogen, which is a major constituent of all three points (as discussed earlier).

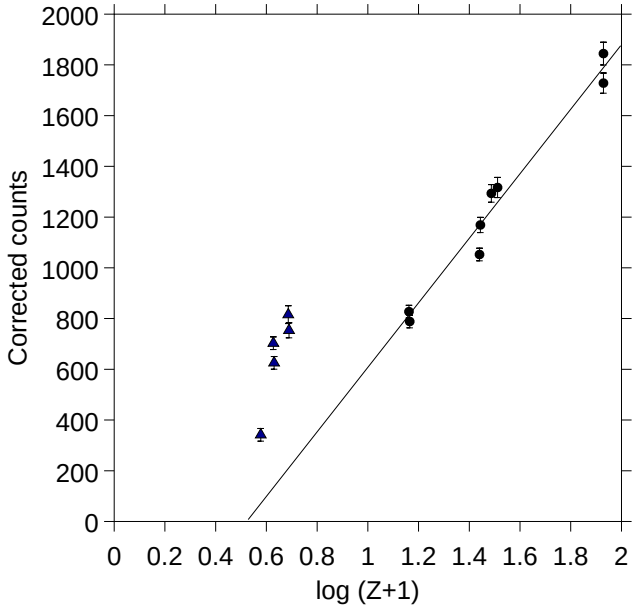


**Fig. 15.** The fourth plot of the $Z$ dependence of backscattering. The regression line drawn is the best fit of the element points only. Elements are denoted by a circle while compounds are marked by a triangle. This graph again demonstrates that the higher points on the graph are more accurately fitted by the regression line than the lower hydrogen containing points. None-the-less it appears plausible that some connection between the average $Z$ number of simple compounds and their associated backscattering exists.

explanation of the counts from the compounds. The phosbronze has a larger calculated $Z$ number and fits the line reasonably well but the compounds with smaller $Z$ numbers appear quite remote from the line. This can be explained to some extent by referring

to Fig. 12 where there are counts on both carbon graphite and polythene. The point to note is that although the ratio of hydrogen to carbon in polythene is 2 : 1, the polythene points are only just lower than that of the pure carbon. This suggests that hydrogen may not fit the $\log(Z+1)$ relationship very well. This is not unreasonable as the relationship is only an empirical one and hydrogen being the lowest extreme would be the most likely point not to fit. What is interesting is that if the $\log(Z+1)$ calculation for the calcite and copper sulphate is performed without adding in the water of crystallization the values are respectively, 1.01 and 1.09, which are exceedingly close if they do not intersect the line.

## 5. Conclusion

The angular dependence of $\beta$-particle backscattering has been clearly shown to form a linear relationship over the range that was used. This does in fact agree well with the published ideas on the subject, which tend favour a relationship with a cosine fit, as the curve is very closely linear over the range that was used in the experiments.

The $Z$ dependence of $\beta$ backscattering is a subject with little research background yet it was certainly obvious that for elemental scattering samples that they fitted a logarithmic relationship. The $\log(Z+1)$ relationship was an improvement when simple compounds were added to the scattering samples. The graphs showed that the compounds must follow some sort of a similar relationship but calculating a $\log(Z+1)$ value for some of them proved inaccurate, mainly due to the fact that hydrogen atoms seemed to have less influence than the relationship suggested.

Both of these subject areas are heavily lacking in any published data and all relationships that do exist are of an empirical nature. This is not surprising as the idea of single scattering is amenable to calculation but by using a thick sample to achieve backscattering, the multiple scattering of the $\beta$-particles that becomes possible prevents any further theoretical treatment of the subject.

The inaccuracies in the experiments could be greatly reduced by the use of more dedicated equipment that has been specially designed for a particular experiment although to go in search of such minimization was outside the scope of this investigation.

## Acknowledgments

I would like to thank the physics staff and technicians for their help and patience especially when I was looking for obscure scattering samples in the store. I would also like to extend my thanks to the University of Edinburgh Physics Department for allowing me to use the First Year laboratories and equipment.

## Appendix A

In general all errors that are shown in results tables are the total of all errors for a specific measurement and are also be included in any graph of the results. The only exception is where the errors are small enough to be included inside the diameter of the points plotted on the graph.

Errors in $\beta$-particle counting are calculated from the Poisson distribution nature of the counts. Thus a count of $n$ in a particular time period has an associated standard deviation of $\sqrt{n}$.

Furthermore if the background is $b$ measured in time $t_b$ and the count $n$ is over time $t_c$, then the error in the corrected count can be found to be

$$E = \sqrt{(n + bt^2)} \quad \text{where} \quad t = t_c/t_b.$$

Added to this value (if it is significant) is an error associated with a total path distance between the source and the G–M tube. This error is approximate as it is calculated

from the graph of the transmission of the $\beta$-particles through air. The error in the positioning of any object is half of one scale division of the instrument used for the measurement. Generally in this investigation this error is $\pm 0.5$ mm and thus for most of the experiments the total distance error is $\pm 2.0$ mm split between: 0.5 mm for each of the source and G–M tube, and 1.0 mm for the scattering material (it is counted twice since its positioning changes two distances). Using this error in distance in conjunction with the graph mentioned and over the limits, $0.05\ m <$ separation $< 0.4$ m, an error in the count due to the error in positioning can be found, which is generally of the order of 5%.

The value of the error in the angular measurement is taken as the angle subtended by the G–M tube. That is to say, the inverse tan of the radius of the tube (9.5 mm) divided by the distance to the scattering material.

## Appendix B
## Gaussian distribution of $\beta$ disintegration measurements

This experiment was performed as a demonstration of the normal approximation to the Poisson distribution of measurements of $\beta$-particle disintegrations [7]. This leads to the standard deviation in the count being equal to the square root of the count as discussed in Appendix A. The idea was to take twenty measurements of the number of disintegrations from the $^{90}$Sr source over a time duration and separation that would give counts of around 100. The experiment were then repeated using a duration ten times the size so as to obtain counts of around 1000.

For clarity the results are not included; instead the results are represented as histograms of the number of counts in each standard deviation away from the mean (Fig. 16). Plotted alongside each bar is the expected number of counts calculated using the Gaussian distribution. For the purposes of these results the percentage deviation is percentage difference in the expected count when one moves one standard deviation away from the mean.

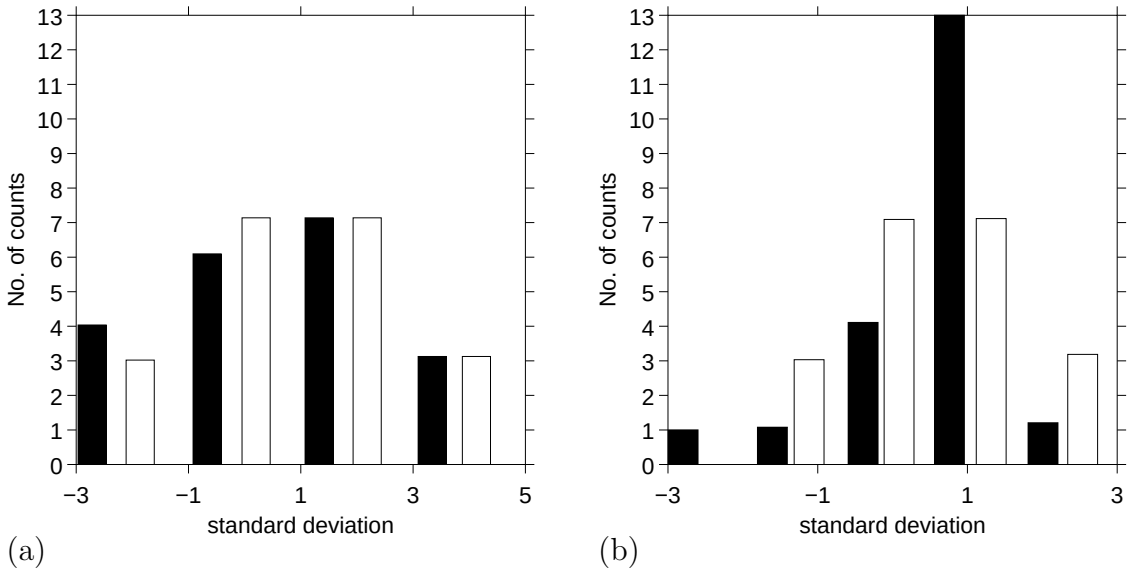


**Fig. 16.** The plots demonstrate the Gaussian distribution of $\beta$ disintegration measurements. Plot (a) is measured over 30 s; plot (b) is measured over 300 s.

For the counts taken over 30 s the mean of the results is 119 with standard deviation 11. Therefore the percentage deviation in these results is

$$100 \times 11/119 \approx 9\%.$$

For the counts taken over 300 s the mean of the results is 1089 with standard deviation 33. Therefore the percentage deviation in these results is

$$100 \times 33/1089 \approx 3\%.$$

Thus by comparison with the 30 s results it is clearly demonstrated that by increasing the size of the count, the spread about the mean is reduced greatly.

# References


[1] J. Yarwood, *Electricity, Magnetism, and Atomic Physics*, Vol. 2, University Tutorial Press, London 1958, p. 383

[2] M. Brucer, *Trilinear Chart of the Nuclides*, Mallinckrodt Nuclear, St. Louis 1968

[3] F. Tyler, *A Laboratory Manual of Physics*, 6th ed., Edward Arnold, London 1988, p. 247

[4] G. Knop, W. Paul, in: $\alpha$ $\beta$ $\gamma$ *Ray Spectroscopy*, Ed. K. Seigbahn, Vol. 1, North-Holland, Amsterdam 1966, p. 1

[5] H.A. Bethe, M.E. Rose, L.P. Smith, Proc. Amer. Phil. Soc. **78**, 573 (1938)

[6] N.A. Baily, Med. Phys. **7**, 514 (1980)

[7] G.L. Squires, *Practical Physics*, McGraw-Hill, London 1968, p. 200